Implementation of a nonlinear elastoplastic model for tunneling in sandstone

Fu-Husan Yeh[1], M.-C. Weng[2], and L. Ge[1]

[1] Department of Civil Engineering, National Taiwan University, 1, Sec.4, Roosevelt Rd., 10617, Taipei, Taiwan 300, R.O.C.
[2] National Chiao Tung University, 1001 University Road, Hsinchu, Taiwan 300, R.O.C.

ABSTRACT

The most active infrastructure constructions for transportation take place in the western Taiwan due to dense population. Hillside development is a vital issue for urban planning. Adequate understanding of sedimentary rocks, e.g. sandstone, mostly weak rock, plays an important role in the construction of tunnels; therefore, properly evaluating deformation of rock is essential. To mimic the deformation characteristics of sandstone, such as shear stress and volumetric strain coupling behavior, a nonlinear elastoplastic model based on the theory of Green elasticity and generalized plasticity has been implemented into finite element code ABAQUS through user-defined subroutine UMAT. A series of triaxial tests of a single element are first simulated to verify the model. After the verification, excavation of a tunnel is simulated under plain stain condition. This study concludes that the model is capable of describing the deformation characteristics of tunnel excavation in sandstone and provides a valuable tool for future engineering practice.

Keywords: sandstone; tunnel; elastoplastic model

1 INTRODUCTION

The western region of Taiwan is most populous and accompanied by active constructions of transportation infrastructures. Many tunnel constructions currently in progress or under planning are, or to be, constructed in sedimentary strata formed in the Tertiary Period. Due to the relatively young rock-geneses period and possibly other factors, these sedimentary strata are found mostly weak rocks. In the past, these weak rocks have caused several engineering difficulties such as shear-induced squeezing and creeping deformations during tunnel construction. Through a series of laboratory triaxial tests, it was found that some typical weak rocks exhibit problematic characteristics such as substantial wet weakening, shear-dilation as well as creep deformation. Such behavior is often much less significant in hard rocks. To understand the key behaviors and to rationally predict the deformation for design, this study aims to implement a constitutive model, proposed by Jeng et al. (2017), which can mimic these problematic deformational behaviors in finite element software for engineering practice.

The adopted model is a nonlinear elastoplastic model. The elastic component is based on the theory of Green elasticity while the plastic component is based on generalized plasticity. It can be used to simulate strain hardening and strain softening behavior. In addition, it is implemented into finite element software ABAQUS through user-defined subroutine UMAT.

To verify the model validity in ABAQUS, a series of triaxial tests of a single element are first simulated. After the validation, the excavation of a tunnel is simulated using plain stain analysis. Meanwhile, other constitutive models are also adopted for comparison.

The deformation of rock material was usually simulated by isotropic linear elastic model with Drucker-Prager or Mohr-Coulomb constitutive models; however, these models were not appropriate to describe the characteristics of the deformation of sandstone, such as a nonlinear elastic deformational behavior under different volumetric stresses, and the coupling behavior between shear stress and elastic volumetric strain under varying shear stresses. Some post numerical researches on the deformational behaviors of tunnel excavation in weak rock have been carried out. (e.g., Jongpradist et al., 2004; Chen et al., 2011; Zhou et al., 2014, etc.).

2 THE CONSITITUTIVE MODELS

A constitutive model proposed by Weng (2014) and Jeng et al. (2017) is used in order to simulate the behavior of sandstone. The total strain increment can be divided into elastic and plastic components as follows:

$$d\boldsymbol{\varepsilon} = d\boldsymbol{\varepsilon}^e + d\boldsymbol{\varepsilon}^p \tag{1}$$

where $d\boldsymbol{\varepsilon}$, $d\boldsymbol{\varepsilon}^e$, and $d\boldsymbol{\varepsilon}^p$ are the increments of total, elastic, and plastic strain tensors, respectively.

The increments of elastic and plastic strain can be calculated as below:

$$d\boldsymbol{\varepsilon}^e = \mathbf{C}^e : d\boldsymbol{\sigma} \tag{2}$$

and

$$d\boldsymbol{\varepsilon}^p = d\lambda \mathbf{n}_g = \frac{1}{H_{L/U}} \left(\mathbf{n}_{gL/U} \otimes \mathbf{n} \right) : d\boldsymbol{\sigma} \tag{3}$$

where $\boldsymbol{C}^e$ is the elastic constitutive tensor, $d\boldsymbol{\sigma}$ is the increment of the stress tensor, $\boldsymbol{n}_g$ is the unit tensor defining the plastic flow direction, $\boldsymbol{n}$ represents the loading-direction tensor, $d\lambda$ is a plastic scalar, and $H_{L/U}$ is the plastic modulus, which can be assumed directly without introducing a hardening rule. Subscripts L and U indicate loading and unloading, respectively.

In finite element analysis, usually, the increment of stress as a function of the strain increment is utilized; therefore, Eq. (2) is inverted and expressed as

$$d\boldsymbol{\sigma} = \boldsymbol{D}^{ep} : d\boldsymbol{\varepsilon} \tag{4}$$

and

$$\boldsymbol{D}^{ep} = \boldsymbol{D}^{e} - \frac{\boldsymbol{D}^{e} : \boldsymbol{n}_{g_{L/U}} \otimes \boldsymbol{n} : \boldsymbol{D}^{e}}{H_{L/U} + \boldsymbol{n} : \boldsymbol{D}^{e} : \boldsymbol{n}_{g_{L/U}}} \tag{5}$$

where $\boldsymbol{D}^{ep}$ and $\boldsymbol{D}^{e}$ are the elastoplastic and elastic matrix, respectively.

This generalized plasticity model has the advantage that the yield and potential surfaces are not directly defined, but only the scalar functions for plastic modulus $H_{L/U}$, direction tensors $\boldsymbol{n}$, and $\boldsymbol{n}_g$, are required. The adopted model can incorporate the deformation characteristics of sandstone into generalized plasticity by subsequently defining nonlinear elasticity, dilatancy, and plastic modulus.

2.1 Nonlinear Elastic Behavior

According to Green elasticity theory, the strain tensor is related to the derivatives of the energy density function in the following:

$$\boldsymbol{\varepsilon}^e = \frac{\partial \Omega}{d\boldsymbol{\sigma}} \tag{6}$$

where Ω is the energy density function.

Based on experimental sandstone results, this study adopts the following energy density function for Ω, which has been proposed by previous studies (Weng, 2014):

$$\Omega = b_1 I_1^{3/2} + b_2 I_1^{-1} J_2 + b_3 J_2 \tag{7}$$

where b_1, b_2, and b_3 are material parameter which are used to present elastic behavior, I_1 is the first stress invariant (I_1 = 1/3$\boldsymbol{\sigma}$:$\boldsymbol{\sigma}$ = 3P'), and J_2 is the second deviatoric stress invariant (J_2 = 0.5$\boldsymbol{S}$:$\boldsymbol{S}$, where $\boldsymbol{S}$ is the deviatoric stress tensor). After substituting Eq. (7) into Eq. (6), the elastic strain tensor $\boldsymbol{\varepsilon}^e$ can be presented as follows:

$$\boldsymbol{\varepsilon}^e = \frac{\partial \Omega}{\partial \boldsymbol{\sigma}} = (\tfrac{3}{2} b_1 I_1^{1/2} - b_2 I_1^{-2} J_2 + J_2)\boldsymbol{\delta} + (b_2 I_1^{-1} + b_3)\boldsymbol{S} \tag{8}$$

where $\boldsymbol{\delta}$ is the Kronecker delta tensor.

2.2 Dilatancy and Viscoplastic Flow

For stress-dilatancy relationships, the function is expressed in the following form, which is similar to the function proposed by Pastor et al. (1990).

$$d_g = \frac{d\varepsilon_v^p}{d\gamma^p} = (1+\alpha)(M_g - \eta) \tag{9}$$

where $d\varepsilon_v^p$ and $d\gamma^p$ are incremental plastic volumetric and shear strains, respectively. The term M_g is the threshold of shear dilation in the triaxial plane. When $\eta = M_g$, d_g equals zero and volumetric strain does not occur. The sandstone converts from compression to dilation when $\eta > M_g$. Variable α is a model parameter.

Based on the definition by Weng and Ling (2012), the stress ratio η is defined as

$$\eta = q / q_f \tag{10}$$

where $q = \sqrt{3J_2}$, and q_f is the shear strength. Drucker-Prager criterion is adopted to present the linear strength criterion as Eq. (11):

$$q_f = \sqrt{3J_{2f}} = \sqrt{3}(\alpha_d I_1 + k_d) \tag{11}$$

where parameters α_d and k_d are the slope and cohesive intercepts of the failure envelope, respectively.

According to Pastor et al. (1990), the plastic flow direction under loading and unloading $\boldsymbol{n}_{gL/U}$ in the triaxial space is

$$\boldsymbol{n}_{gL/U} = \left(\frac{d_g}{\sqrt{1+d_g^2}}, \frac{1}{\sqrt{1+d_g^2}}\right)^T \tag{12}$$

Similarly, the loading-direction tensor can be expressed as

$$\boldsymbol{n} = \left(\frac{d_f}{\sqrt{1+d_f^2}}, \frac{1}{\sqrt{1+d_f^2}}\right)^T \tag{13}$$

where $d_f = (1+\alpha)(M_f - \eta)$ and M_f is a material parameter.

According to Jeng et al. (2002) and Weng et al. (2005), the triaxial results showed that the plastic potential surface of sandstone coincides with the yield surface in the pre-peak stage. Therefore, the associated flow rule, $\boldsymbol{n} = \boldsymbol{n}_{gL/U}$ and $M_f = M_g$, can be used when formulating the constitutive model for sandstone. To consider the post-peak behavior, $\boldsymbol{n}$ might be different from $\boldsymbol{n}_{gL/U}$ which means that the non-associated flow rule is followed. However, the associated flow rule is used to simplify the adopted model in this study.

2.3 Plastic Modulus for Loading and Unloading

2.3.1 Strain Hardening

Let's assume that the post-peak behavior of sandstone is strain hardening, the function of the plastic modulus under loading can be expressed as

$$H_L = H_0 \sqrt{p' / p_{atm}} H_f H_s \tag{14}$$

$$H_f = \left(1 - \eta^2\right) \tag{15}$$

$$H_s = \exp\left(-\beta_0 \xi_s\right) \tag{16}$$

2.3.2 Strain Softening

For simulating strain softening of sandstone behavior, the plastic modulus H_L turns to negative after the peak is reached. And, the H_L, H_s, and H_v need to be changed to the Eq. (17) to Eq. (19), respectively.

$$H_L = H_0 \sqrt{p' / p_{atm}} H_f (H_s + H_v) \tag{17}$$

$$H_s = \exp\left(-\left(\frac{p'}{p_{atm}}\right)^{\beta_0} \xi_s\right) \tag{18}$$

$$H_v = \beta_1 - \frac{q}{p'}\beta_2 \tag{19}$$

where $\xi_s = \int \left| d\gamma^p \right| = \int d\xi_s$ is the accumulated plastic shear strain, H_0 is a multiplication factor related to the initial plastic modulus, H_f, H_s, and H_v are plastic coefficients, P_{atm} is the atmospheric pressure, and β_0, β_1, and β_2 are material parameters.

To consider the plastic strains occur during the unloading process; the unloading plastic modulus H_u can be expressed as

$$H_u = H_{u0} \tag{20}$$

where H_{u0} is a material parameter.

3 MODEL VALIDATION AND SIMULATION

3.1 Triaxial Tests of MS Sandstone

There is a total of twelve material parameters (b_1, b_2, b_3, α_d, k_d, M_g, α, H_0, β_0, β_1, β_2, H_{u0}) need to be determined. The detailed parameter determination refers to Jeng et al. (2017).

The triaxial tests of a single element are first simulated in order to verify the validity of the model in ABAQUS. Table 1 shows the parameters of the simulations. The results show that the simulations agree well with laboratory tests as shown in Fig. 1 to Fig. 4.

3.2 Tunnel Excavation Simulation

The model is used to simulate a tunnel excavation as shown in Fig. 5, which is a tunnel at Northern National Highway No.2. The overburden depth to the top of the tunnel is about 60 m, the height of tunnel is 11.4 m, the width of the tunnel is 16 m, and the unit weight is 25 kN/m^3. To consider the side effects of the simulated model, the size of the simulation model is 160 m×200 m. Plain stain analysis is applied. In this simulation, the constitutive models of strain hardening and strain softening are adopted. Meanwhile, other constitutive models are also taken into consideration for comparison, including elastic and Drucker-Prager.

Generally, the strength of this kind of weak rock is relatively low. In this study, excavation sequence is considered. The following lists the procedures for numerical analysis. It is divided into the following steps:

(1) The geostatic step is used to balance the stress field before excavation. It is used to simulate the tectonic stress. The lateral coefficient K_0 is assumed as 1.
(2) Excavate the top heading. And, excavate the bench.

This model is used to analyze the deformations and the risk factors after excavation under the different constitutive models. The parameters for the engineering case study are listed in Table 2.

The deformation behavior of rock mass around tunnel is determined by deducting the relative displacement of the rigid body deformation after tunnel excavation. The results show that the deformation of the study of strain hardening and strain softening are higher than elastic and Drucker-Prager constitutive models in Table 3. The reason might be that substantial wet weakening, shear-dilation as well as creep deformation are effective within the adopted models..

Besides, to compare the risk factors between the adopted models of strain hardening and strain softening in Fig. 6, the range of risk factors of softening mode is wider than hardening mode because the softening mode allows more plastic strain to develop than hardening mode when the stress starts to decrease.

The simulation exhibits that the model of strain softening is capable of describing the deformation characteristics of sandstone, such as shear stress and volumetric strain coupling behavior. Especially, the strain softening behavior of the rock is more adequate to present the engineering practice.

4 CONCLUSION

The characteristics of sandstone including strain-stress curve on the stage of confining and deviatoric stress agree well with the series of laboratory triaxial tests. The results show that the nonlinear elastoplastic model is successfully implemented in ABAQUS using the UMAT. Using the nonlinear elastoplastic model to predict deformation of a tunnel in sandstone is acceptable; moreover, the strain softening of the adopted model is more suitable to present the engineering practice. It provides a valuable analysis resource in the near future.

REFERENCES

Chen, X., Guo, H., Zhao, P., Peng, X., Wang, S. (2011). Numerical modeling of large deformation and nonlinear frictional contact of excavation boundary of deep soft rock tunnel, Journal of Rock Mechanics and Geotechnical Engineering, 3, Supplement 1, 421-428.

Jeng, F. S., Weng, M. C., Huang, T. H. and Lin, M.L. (2002). Deformational Characteristics of Weak Sandstone and Impact to Tunnel Deformation, Tunnelling and Underground Space Technology, 17, 263-264.

Jongpradist, P., Takeuchi, K., Shimura, T. & Horii, H. (2004). Rock Mass Deformational Behaviors during the Excavation of the Large-scale NATM Cavern in Soft Sedimentary Formation, J. Geotech. Eng., JSCE, No. 764/III-67, 1-10.

Jeng, F. S., Weng, M. C., Yeh, F. H., Yang, Y. H., & Huang, T. H. (2017). A Constitutive Model of Sandstone Considering the Post Peak Behavior. Journal of Mechanics, 1-13.

Pastor, M., Zienkiewicz, O. C., and Chan, A. H. C. (1990). Generalized Plasticity and the Modelling of Soil Behavior, International Journal for Numerical and Analytical Methods in Geomechanics, 14, 151-190.

Weng, M. C., Jeng, F. S., Huang, T. H. and Lin, M. L. (2005). Characterizing the Deformation Behavior of Tertiary Sandstones, Int J Rock Mech Min Sci, 42, 388-401.

Weng, M. C. and Ling, H. I. (2012). Modeling the behavior of sandstone based on generalized plasticity concept. Int. J. Numer. Anal. Meth. Geomech. DOI: 10.1002/nag.2127

Weng, M. C. (2014). A Generalized Plasticity-Based Model for Sandstone Considering Time-Dependent Behavior and Wetting Deterioration, Rock Mechanics and Rock

Engineering, 47, 1197-1209.

Zhou, H., Zhang, C., Li, Z., Hu, D., Hou, J. (2014). Analysis of mechanical behavior of soft rocks and stability control in deep tunnels, Journal of Rock Mechanics and Geotechnical Engineering, 6(3), 219-226.

Table 1. Parameters of single element simulation

Material Properties	Parameters	Mushan Sandstone (MS)
Elastic	b_1 (MPa)$^{-1/2}$	130×10^{-6}
	b_2	1463×10^{-6}
	b_3 (MPa)$^{-1}$	29×10^{-6}
Failure Envelopes	α_d	0.39
	k_d (MPa)	8.2
Plasticity	M_g	0.62
	α	2.9
	H_0 (MPa)	4590
	β_0	120
	H_{u0} (MPa)	180,000

Table 2. The parameters for the engineering case study

Constitutive model	Mass Parameters		
Elastic	Elasticity, E (MPa)		200
	ν		0.21
Drucker-Prager	Elasticity, E (MPa)		200
	ν		0.21
	k_d (kPa)		82
	α_d		0.2
The study of strain hardening	Elastic	b_1 ((MPa)$^{1/2}$)	0.002
		b_2	0.03
		b_3 ((MPa)$^{-1}$)	0.005
	Failure Envelopes	α_d	0.2
		k_d (MPa)	0.082
	Plasticity	Mg	0.62
		α	2.9
		H_0 (MPa)	316
		β_0	120
The study of strain softening	Plasticity	Mg	0.62
		α	1.6
		H_0 (MPa)	1106.8
		β_0	2
		β_1	0.6
		β_2	0.65

Table 3. The comparisons of deformations under different constitutive model analysis after tunnel excavation

Squeeze deformation	Crown (cm)	Invert (cm)	Right side (cm)
Elastic Model	-10.45	8.71	-5.62
Drucker-Prager Model	-17.23	18.02	-8.99
The study of strain hardening	-20.06	16.86	-10.72
The study of strain softening	-21.63	19.54	-12.64

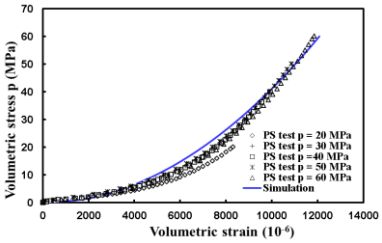

Fig. 1. Simulation results of volumetric stress versus volumetric strain curve under different confining pressures

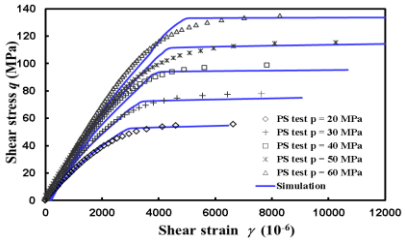

Fig. 2. Simulation results of shear stress versus shear strain under the different confining pressures

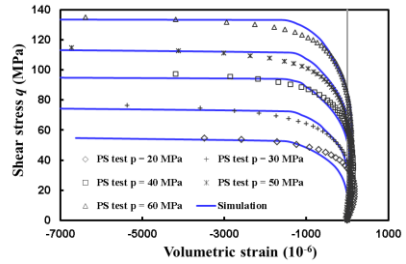

Fig. 3. Simulation results of shear stress versus volumetric strain under the different confining pressures

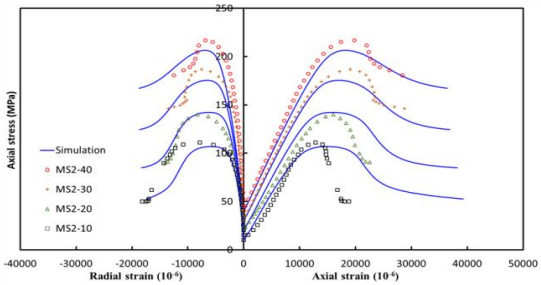

Fig. 4. The strain softening simulation

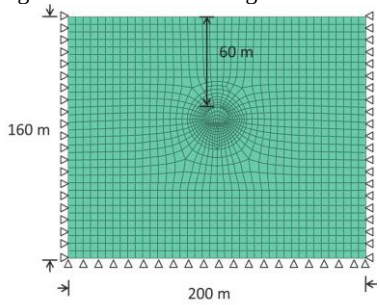

Fig. 5. A model for tunnel excavation simulation

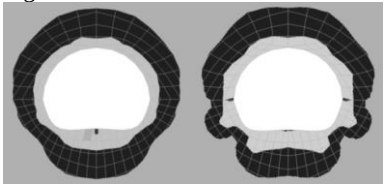

(a) Strain hardening (b) Strain softening

Fig. 6 Comparison of the risk factors from the two adopted models